Influence of texture on dynamic recrystallization and deformation mechanisms in rolled or ECAPed AZ31 magnesium alloy

J. A. del Valle, O. A. Ruano

Department of Physical metallurgy, CENIM, CSIC, Av. Gregorio del Amo 8,

28040 Madrid, Spain.

Abstract

Equal channel angular pressing (ECAP) and hot rolling are widely used processing routes in magnesium alloys. These routes induce different textures that affect their mechanical properties. In the present work, the influence of the texture on dynamic recrystallization (DRX) and deformation mechanisms was investigated. During tensile deformation at moderate temperatures, a stronger enhancement of DRX in rolled samples than in ECAPed samples is observed. Simultaneously, in both samples, texture evolves towards a deformation texture consisting of a basal fibre with directions $\langle 01\bar{1}0 \rangle$ parallel to the tensile axis. The deformation delay for the start of DRX of ECAPed samples can be consistently related to the strain necessary to develop this fibre. It is assumed that the fibre texture stimulates DRX through the enhancement of multiple slip, which increases heterogeneities of the substructure.

Keywords: Magnesium alloys; Texture; Hot working; Dynamic recovery; Dynamic recrystallization

1. Introduction

Magnesium alloys have attracted great interest due to their excellent specific properties that make them potentially suitable candidates for replacing heavier materials in some automobile parts. Since the seminal work of Ion et al., [1] dynamic recrystallization (DRX) in magnesium alloys has been studied by an increasing number of researchers. Several DRX

mechanisms have been proposed depending on temperature and deformation conditions. These studies reveal the complexity of the process.

Ion et al studied DRX in extruded magnesium compressed in parallel to the basal planes in the range of temperatures 423 to 593 K. A DRX mechanism was proposed consisting of a succession of twinning, basal slip and lattice rotations at grain boundaries forming subgrains and finally recrystallized grains with high angle boundaries. Because this mechanism of DRX consists in a progressive rotation of subgrains is termed rotational recrystallization (RDRX). Moreover, Humphreys et al. [1,2] claim that during this process little boundary migration occurs and no clear division between nucleation and growth can be established. Therefore, this mechanism is included inside the group of continuous recrystallization (CDRX) mechanisms. Ion et al did not find a relationship between DRX grain sizes and steady state flow stress. Moreover, Humphreys and co-workers [1, 2] recognized that, during straining at higher temperatures, discontinuous dynamic recrystallization (DDRX) occurs in the same materials, the temperature for changing mechanisms being close to 600 K [1]

Galyev et al. [3] and Sitdikov and Kaibyshev [4] make an effort to correlate the deformation mechanism with the DRX mechanism. The main conclusion of this work is that CDRX is linked to deformation controlled by cross-slip while DDRX is related to deformation controlled by climb, these deformation mechanisms being inferred from activation energies. The DRX mechanisms of the AZ31 alloy were analyzed by McQueen and co-workers from 453 to 723 K using torsion tests [5, 6]. Differing from Galyev et al., in this case a climb process, with an activation energy close to that for self diffusion, Q_{self}, was found to control creep in the whole range of temperatures [3]. McQueen et al. emphasized the role of dynamic recovery (DRV) in forming the substructure,and the and the role of the microstructure heterogeneities, arising from twinning and multiple slip, on inducing DRX nuclei.

The influence of deformation mode and microstructure on stress-strain behavior and DRX in the AZ31 alloy was investigated by Barnett and co-workers [7, 8, 9, 10]. Barnett et al. found that the progress of recrystallization was sensitive to changes in orientation in relation to the compression axis [7]. Moreover, the lowest recrystallized volume fraction corresponds to a "c-axis constraint" orientation that is mechanically similar to testing a rolled sample in tension along the rolling direction because in both cases prismatic slip is favored. Barnett attributes this behavior to the predominance of prismatic slip favored in detriment of twinning [7, 8]. Although the DRX volume fraction depends on deformation conditions, the recrystallized grain size, d_{rec}, is less sensitive to deformation conditions. Interestingly, the dependence of d_{rec} on the stress is through a lower exponent, when compared with Derby´s analysis [11]. The analysis performed in these works is generally based on the framework of the DDRX theory. The activation energy was found to be close to Q_{self} at 573 K and almost independent of deformation mode and texture.

The DRX under tensile deformation of the AZ31 alloy with a basal texture condition has been studied recently by Yi et al. [12] from room temperature to 523 K. At 423 K, an increase of misorientation from the grain centre towards the grain boundaries is observed. This result is interpreted as evidence of RDRX. At higher temperatures, small DRX grains having a small misorientation between them replace large grains. The formation of a strong texture coincident with the expected deformation texture is attributed to the similar orientation of the new grains (characteristic of CDRX) and, secondly to subsequent straining of the new grains restoring the deformation texture.

The aim of the present study is to investigate the DRX behavior in a commercial Mg-alloy AZ31 with two different processes: rolling and ECAP. The orientation of the basal planes with respect to the tensile axis is different for samples obtained by both process. In the case of ECAP, basal slip is favored while in rolled samples a larger contribution of prismatic

slip is expected under tension in the RD direction. Moreover, these two orientation conditions do not favor the deformation by twinning which has been related to low temperature DRX (LTDRX) and is proved to have a great influence on DRX. Therefore, this study of samples with these specific textures can help to clarify the DRX mechanisms and contributes, therefore, to the above discussion.

In the following, the microstructure and texture changes with deformation are first analyzed. Secondly, the relation of the deformation mechanism with texture is investigated. Taking into account that DRX mechanisms and deformation mechanisms are possibly related, and expecting that texture affect both, this investigation helps to give a consistent explanation of the deformation behavior. Finally, the connection between DRX and texture is discussed at the onset of DRX and during successive deformation.

2. Experimental Procedure

The material used in this study was a commercial Mg alloy AZ31 with the following composition: 3%Al, 1%Zn, 0.2%Mn and Mg (balance), provided by Magnesium Elektron in the form of a sheet, 3 mm in thickness. The alloy was received in the condition AZ31-O (rolled and annealed). These samples are henceforth termed R-samples.

The ECAP processing of the AZ31 alloy consisted of two passes in total, at 523 K, using a square die of 12x12 mm, with an intersection angle of $\Phi = 90^{o}$ and a plunger speed of 0.1 mm/s. Slabs of 3 mm in thickness were stacked, as shown in Fig. 1 of Ref [13], in order to perform the ECAP process. The die was heated in-situ during the ECAP process and the temperature of the die was maintained stable at 523 K. The ECAP process was carried out by route C the stack being rotated 180^{o} around the extrusion direction, ED, of the first pass. Subsequently, the processed AZ31 samples were annealed 120 min at 723 K in order to produce a coarsening of the grain size to values close to those for R-samples. These samples

are henceforth termed EC-samples. The final grain size of the samples EC and R is in the range of 25-30 μm.

The microstructures of the alloy in the different stages of processing were examined by optical microscopy (OM). Sample preparation consists of grinding with a SiC paper, followed by mechanical polishing with 6μm and 1μm diamond paste and short final polishing using colloidal silica. Subsequent etching using a solution of ethanol (100 ml), picric acid (5 g), acetic acid (5 ml) and water (10 ml) revealed the grain structure.

The grain size was determined by means of the linear intercept method, measuring about 1000 grains. The mean recrystallized grain size, d_{rec}, was calculated from the mean intercept length using a 1.74 factor. In the case of low recrystallized volume fraction, d_{rec} was measured from the diameters of individual grains using a factor $4/\pi$ related to probability of cutting a section of a spherical grain. The recrystallized volume fraction, f_{rec}, was determined by the point counting method where points on grains larger than the recrystallized grain size d_{rec} were considered as not recrystallized. Texture measurements were performed in the back-reflection mode by X-Ray diffraction using an X-Ray diffractometer with HI-STAR two dimensional multiwire proportional counters (General Area Detector Diffraction System, Bruker AXS). Co K_α radiation was employed at a tube current of 30 mA and a voltage of 40 KV. The detector was centered at $2\theta = 40.2^o$, 62.0^o and 78.3^o, with the center of the detector 2θ position coupled with the beam´s incident angle θ. At each 2θ position enough planar frames were collected for covering the entire pole sphere. From the normalized and corrected data, the pole figures were constructed.

Dog-bone tensile samples of 15 mm gage length and a radius of 3 mm were machined out of the R and EC slabs with the tensile axis parallel to the rolling and ECAP directions, RD, and ED, respectively. Tensile tests were performed in a screw driven testing machine equipped with a parabolic furnace. The testing machine conducts an automatic adjustment of

cross-head speed by compensation of the gauge length increase to maintain constant true strain rates. Continuous tensile tests were conducted at a strain rate of $3x\ 10^{-3}\ s^{-1}$ until fixed strain levels followed by quenching in order to determine the microstructural evolution during DRX.

Additionally, strain rate change tests were carried out at different temperatures as described in Refs. [14, 15], . In this case, the initial strain rate was $5\ x10^{-3}\ s^{-1}$, followed of successive jumps to 10^{-3}, $3x10^{-3}$ and $10^{-2}\ s^{-1}$ once the maximum load is reached.

3. Results

Fig. 1 summarizes the textures of the R and EC samples, termed as "initial textures". As depicted in Fig 1, samples for texture measurements were machined out from transverse sections in the case of EC samples. The rolling texture is basal, with a slight spread. The texture evolution during ECAP was similar to that for the AM60 alloy, analyzed in a previous work [13]. For route C, the (0002) pole figure reveals the formation of a maximum located at 45º from ED towards the transverse direction, TD, indicating that the basal planes rotate during ECAP to a position parallel to the shear direction. As it is well known [16], the operating slip planes after the first pass are favorable oriented for the continuation of the strain in the next ECAP pass by route C. Thus, this particular orientation is reinforced. Therefore, the main difference between the ECAP and rolling samples are the orientation of the basal planes with respect to the tensile axis and the maximum intensities, which are twice in the R samples. It is worth noting that the texture evolution during deformation was also investigated at two test temperatures, 523 and 623 K. For these temperatures, the textures measured on EC samples, after a strain of $\varepsilon = 0.4$, are given in Fig. 1. No change in texture was observed in R-samples and their pole figures are not shown.

Stress-strain curves of R and EC samples at different temperatures in the range 423-623

K are shown in Fig. 2. The maximum stress is marked on top of the curves. In Fig. 3, the flow stress, measured by strain-rate change tests, is plotted as a function of the strain rate.

On the other hand, Fig 4 shows optical micrographs of R and EC samples tested to ε = 0.4 at temperatures in the range 473 to 623 K. Additionally, micrographs at higher magnification for R and EC samples, tested at 423 and 473 K respectively, are shown in Fig. 5. A comparison between $f_{rec}(\varepsilon = 0.4)$ values of R and EC samples as test temperature increases is given in Fig. 6a. In Figure 6b a comparison of the evolution of f_{rec} with strain is also shown for R and EC samples at a constant temperature of 523 K. The recrystallized grain size, d_{rec}, is represented as a function of the maximum stress in Fig. 7a.

5. Discussion

5.1. Evolution of the microstructure during the tensile tests

As it is clearly seen in Fig. 4, DRX is enhanced in R-samples in comparison with EC-samples for equal strains levels. The micrographs at higher magnification of Fig. 5 show the temperatures at which recrystallization becomes evident for R (423 K) and EC (473 K) samples. A minor amount of DRX is observed in both samples near the triple points and the bulging of grain boundaries is also evident.

The enhancement of DRX in R-samples is revealed in Fig. 5 where f_{rec} is plotted as a function of Z and strain for R and EC samples. Figure 6a shows that higher values of f_{rec} are obtained for R-samples than for EC-samples at any given value of Z. In addition, figure 6b shows that f_{rec} is larger for R-samples than for EC-samples at any given value of strain. .

Under increasing test temperature, the differences between R and EC samples remain up to 573K. At the highest temperature analyzed, 623K, the microstructure developed is quite similar in both cases and some grain growth beyond the initial grain size can be also seen, Fig.4.

It is interesting to analyze the relation between the recrystallized grain size, d_{rec}, and the maximum stress, Fig 7. In the first place, there is no significant difference in d_{rec} between R and EC samples. Secondly, there is a well defined relation between grain size and the maximum stress despite that some samples are far from a completely DRX microstructure corresponding to the steady state of recrystallization. A stress exponent of -1.56 is found in the present work, Fig. 7, which correlates very well with the value obtained by Derby on a wide recompilation of metals and minerals [11]. It is noted that Derby's dependence of d_{rec} on stress is typical of materials which undergo DDRX. Our result is quite different from that obtained by Barnett [8] and Guo et al. [17] who obtained an exponent of -0.6. These differences could be attributed to the different test temperatures used in Barnett's work, 573 and 673 K. These two temperatures are too high to keep grain sizes finer than 5 μm, i.e. some metadynamic grain growth could occur. The stability of fine grains can be seen in a recompilation of data on grain growth during annealing treatments in the AZ31 alloy given in Fig. 3 of Ref. [18]. In the present case, the two finer grain sizes of Fig 7 are obtained at 423 and 473 K, micrographs of Fig. 5.

Summarizing, the experimental data show an enhancement of DRX in R-samples in comparison with EC-samples given by an increase in the deformation necessary to obtain a given DRX volume fraction at moderate temperatures. On the other hand, the value of d_{rec} is the same for both types of samples. These effects should be explained based on differences of initial textures.

5.2. Evolution of the texture during the tensile test

Fig. 1 shows pole figures corresponding to R and EC samples after tensile tests carried out to $\varepsilon = 0.4$ at 523 and 623 K.

In R-samples, deformation at 523 and 623 K induce DRX up to $f_{rec} = 0.70$ and ≈ 1

respectively. Despite this relatively extensive DRX only minor variations on the general appearance of the pole figures were found.

Regarding the texture evolution in EC-samples, it should be first considered that deformation at 523 and 623 K induce DRX up to $f_{rec} = 0.2$ and ≈ 1 respectively. Considerable changes in orientation become evident in the case of 523 K where deformation produces a rotation of basal planes towards a position parallel to the tensile axis, Fig.1, developing a basal fibre with the $\langle 01\bar{1}0 \rangle$ aligned with the tensile axis. On the other hand, at 623 K, a less amount of rotation of the basal planes occurs reaching an intermediate position between the initial and that corresponding to deformation at 523 K. This is also the texture evolution expected by deformation on basal planes such that the c-axis becomes normal to the tensile direction.

Yi et al. [19] studied the texture evolution during uniaxial load of samples prepared at different angles from the extrusion direction at room temperature. Samples at 0^o and 45^o shows an evolution of texture to the fibre component $\langle 01\bar{1}0 \rangle$ parallel to the tensile axis. This behavior was rationalized using a texture simulation model. Therefore, this fibre texture can be considered as the deformation texture in the tensile deformation condition on R and EC samples.

However, an effect of DRX on texture is expected according to the RDRX mechanism which predicts defined rotations of new grains relative to old grains. According to Humphreys et al. [1, 2] this DRX mechanism is strongly related to the lack of slip systems. For this reason, the deformation is restricted to basal planes leading to lattice rotations close to grain boundaries forming subgrains and finally recrystallized grains with high angle boundaries. It is expected that deformation carried mostly by basal slip, experimentally achieved in EC-samples, fulfill Humphreys assumptions. Thus, the RDRX mechanism finds, in these samples, the ideal condition to operate. According to the literature [3], this mechanism is expected to

occur at the moderate temperature of 523 K.

It is, therefore, necessary to analyze the expected rotation according to RDRX. In Fig 8 the rotation of recrystallized grains is analyzed in tensile and compressive deformation. Fig 8a shows the original model of Refs. [1, 2] for compression with only one modification: we draw the basal planes with a lower inclination with respect to the compression axis (45^o instead of $\approx 90^o$), because it is more alike to our EC-samples. The scheme of Fig. 8a shows that the slip in the basal planes produces a kinking of the lattice near to the grain boundary and the rotation of basal planes in the new grains is towards a position with the c-axis at higher tilt with respect to the compression axis (basal planes more parallel to the compression axis). In contrast, Fig. 8b shows our case of tensile deformation. The change to tensile conditions produces a similar kink on the lattice, which is in the opposite direction that in compression. In this case, the c-axis rotates towards the tensile axis. Thus, we may expect a different rotation during RDRX depending on stress sign. It is pointed out that this model predicts a rotation that is the opposite of that shown in Fig 1.

Summarizing, while the R-samples have a large amount of DRX with minor changes in the texture, the EC-samples have a low amount of DRX and simultaneously a large amount of changes in texture. This is evidence that DRX is not the cause of the texture evolution. Therefore, the texture evolves, during the tensile test, towards a deformation texture since the changes are related to rotation of the lattice due to slip activity. This explains both the constancy of texture in R-samples and the rotation in EC-samples at 523 K.

4.3. Deformation mechanisms

In the following, the influence of texture on the deformation mechanisms is analyzed. Some researchers argue that the deformation mechanisms affects DRX [3,6]. In sections 4.1 and 4.2, a noticeable influence of texture on DRX was described. Therefore, it is interesting to

analyze if such influence is exerted directly on DRX or the influence is through an alteration of the deformation mechanisms that later influence DRX.

The mechanical behavior of metallic materials during creep at high temperatures is described by the following power law relation between the strain rate, $\dot{\varepsilon}$, and the steady state stress, σ, [20, 21]:

$$\dot{\varepsilon} = A\, D \left(\frac{\sigma}{E}\right)^n \quad (1)$$

where A is a material constant, E is Young's modulus, $D = D_o \exp(-Q/RT)$ is the appropriate diffusion coefficient, Q is the activation energy, R is the gas constant, T is the absolute temperature, and n is the stress exponent.

At large strain rates, or low temperatures, stress exponents larger than 5 are usually found in magnesium alloys [3, 4, 14, 15]. Several specific mechanisms have been proposed, taking into account the measured activation energies, including diffusion controlled dislocation climb and cross-slip controlled slip-creep [3, 4, 5, 22, 23]. Moreover, in some hexagonal metals, Zn [24], and Mg [14], texture effects have been found in this regime.

In a previous work on rolled and ECAPed AM60 alloy [14], it was shown that the texture affects the pre-exponential factor, i.e. the value of A in Eq. (1), without significant changes in the stress exponent. In the present case, Fig. 3, a shift in the curves, that can be attributed to a variation of the pre-exponential factor with texture, can be observed. The EC-samples, with the most favorable orientation for basal slip, are less creep resistant than the R-samples. The data of R samples gives a value of the activation energy, close to that for self-diffusion and constant in the whole range of temperatures. The EC-samples gives values of activation energy close to self-diffusion, except for the activation energy calculated in the transition from 523 to 573 K. This is attributed to variations in the pre-exponential factor A rather to a change in deformation mechanism. In this particular case, if temperature affects the

contributions of the slip systems and these, in turn, affect the value of A, the determination of the activation energy will be made more difficult in light of the usual assumption that A is constant.

On the other hand, a temperature-dependent activation energy in the ZK60 alloy has been reported by Galiyev et al. [3]. These authors determine an activation energy of 92 kJ/mol at lower temperatures, 473 to 523K, claiming that it is associated with cross-slip, while at higher temperatures, 573 to 723K, the activation energy is that corresponding to self-diffusion associated with climb. These authors link cross-slip and climb to CDRX and DDRX respectively. In the present case, no distinction of temperature ranges can be made based on the activation energies. The same activation energy is observed even at low temperatures where restoration mechanisms, consisting of DRV, are thus related to climb [5,6].

Summarizing, the underlying deformation mechanism appears to be independent of texture. Therefore, is concluded that the influence of texture on DRX is not related to an alteration of the deformation mechanisms with a subsequent effect on DRX.

4.4. The relation between the texture evolution and DRX

As mentioned previously, the experimental data show an enhancement of DRX in R-samples in comparison with EC-samples. However, no distinction between these samples can be made based on deformation mechanisms (Section 4.3). Additionally, for both samples, there is evidence that DRX is not the cause of the texture evolution, which consists in the establishment of a deformation texture. The only possible DRX effect on texture is the slight decrease of the fibre intensity for samples tested at 623 K in comparison with samples tested at 523 K.

It is our contention that the opposite relation occurs; i.e., the initial texture and the texture evolution cause the DRX differences between R and EC samples. This connection can

be inferred from the present results at 523 K. On one hand, major DRX is observed in R-samples having fibre texture, and on the other hand DRX is delayed in EC-samples starting to be noticeable simultaneously to the rotation of texture towards the fibre texture. Therefore, it may be claimed that the differences in DRX between R and EC samples are mostly due to a given deformation necessary to produce this rotation. Once the fibre texture is developed in EC-samples, DRX starts to operate. At the higher temperature of 623 K the tendency of these samples to show a similar DRX behavior than that of R-samples could also be related to an increase in multiple-slip in EC samples due to the decrease of the differences in CRSS of the various slip systems.

Therefore, it may be assumed that there is no difference in the underlying DRX mechanism between R and EC samples. This assumption also explains why the recrystallized grain size d_{rec} is almost insensitive to the texture of the samples.

The reason for the basal texture, with the $\langle 01\bar{1}0 \rangle$ direction parallel to the tensile axis, enhancing DRX is probably related to the enforcement of multiple-slip instead of basal single-slip, which is initially favored in EC-samples. According to the literature [2], multiple-slip produces heterogeneities in the dislocation substructure. This usually is associated to the creation of nucleus for DDRX [2]. However, mechanisms based on the continuous development of high angle boundaries, i.e. CDRX or RDRX, cannot be ruled out [1,2,3,5,6].

6. Conclusions

Most of the findings on high temperature deformation analyzed in the present work, including the mechanical behavior and DRX, could be readily explained by the role of multiple-slip. This study highlights the importance of deformation modes on DRX . The major conclusions are the following:

1. The texture has a great influence on DRX of magnesium alloy polycrystals. The

experimental data show an enhancement of DRX in R-samples compared with EC-samples given by an increase in the deformation necessary to obtain a given DRX volume fraction at moderate temperatures. Despite the effect of texture on the amount of DRX, the d_{rec} is almost insensitive to texture of the samples. At high temperatures, DRX tends to be similar in EC and R samples.

2. The underlying deformation mechanism, characterized by the stress exponent and activation energy appears to be independent of texture. Therefore, is concluded that the influence of texture on DRX is not related to an alteration of the deformation mechanisms.
3. During deformation at 523 K, texture evolves towards a deformation texture consisting in a basal fibre with directions $\langle 01\bar{1}0 \rangle$ parallel to the tensile axis. Comparison of the microstructural evolution of EC and R samples demonstrates that this fibre enhances DRX more than the initial texture of EC-samples. The deformation delay for the start of DRX of EC-samples can be congruently related to the strain necessary to develop this fibre. It is assumed that the fibre texture stimulates DRX through the enhancement of multiple slip, which increases the heterogeneities of the substructure.

Acknowledgements

The authors acknowledge financial support from CICYT under program MAT2006-02672 and from the Comunidad Autónoma de Madrid under program NAMEALHEX 2006/60M067. JAV acknowledges support from a Ramón y Cajal contract awarded by the Spanish Ministry of Education and Science.

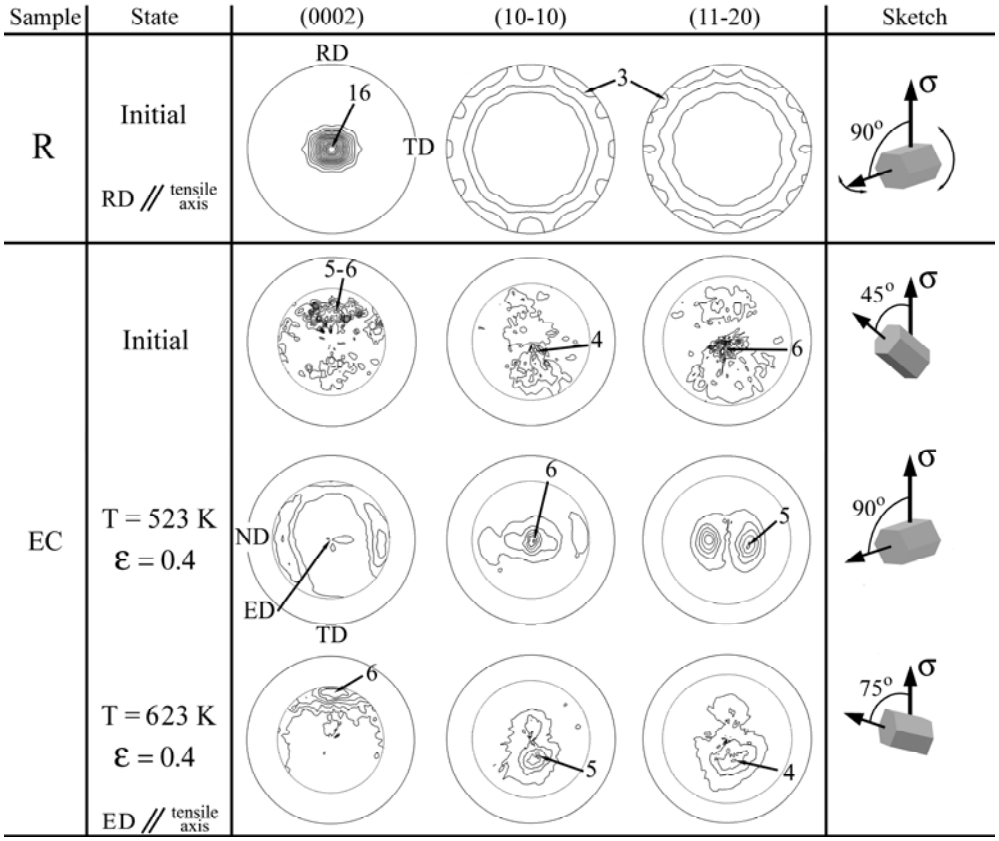

Figure 1: Pole figures of the R and EC samples in the initial state, and deformed to ε = 0.4 at two test temperatures 523 and 623 K.

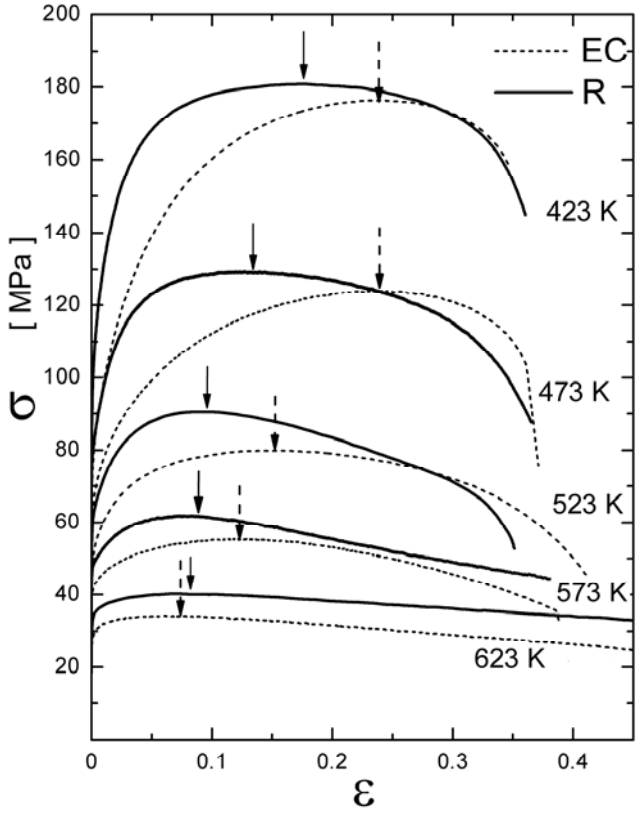

Figure 2: Stress-strain curves of R and EC samples at different temperatures in the range 423-623 K. The deformation to reach the maximum stress, ε_{max}, was marked.

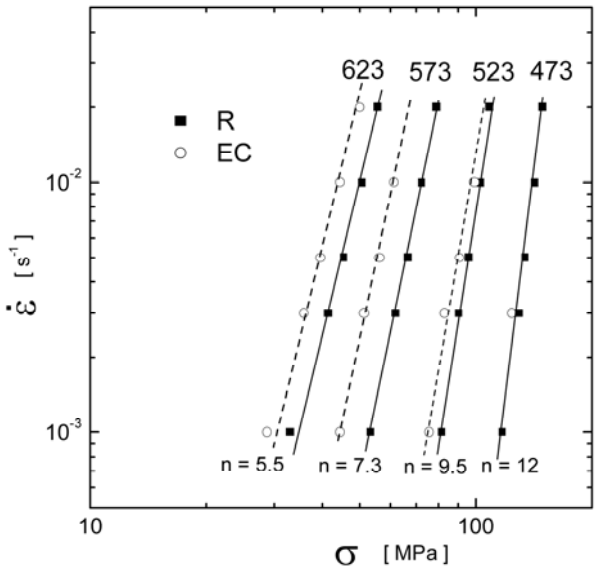

Figure 3: The flow stress is plotted as a function of the strain rate.

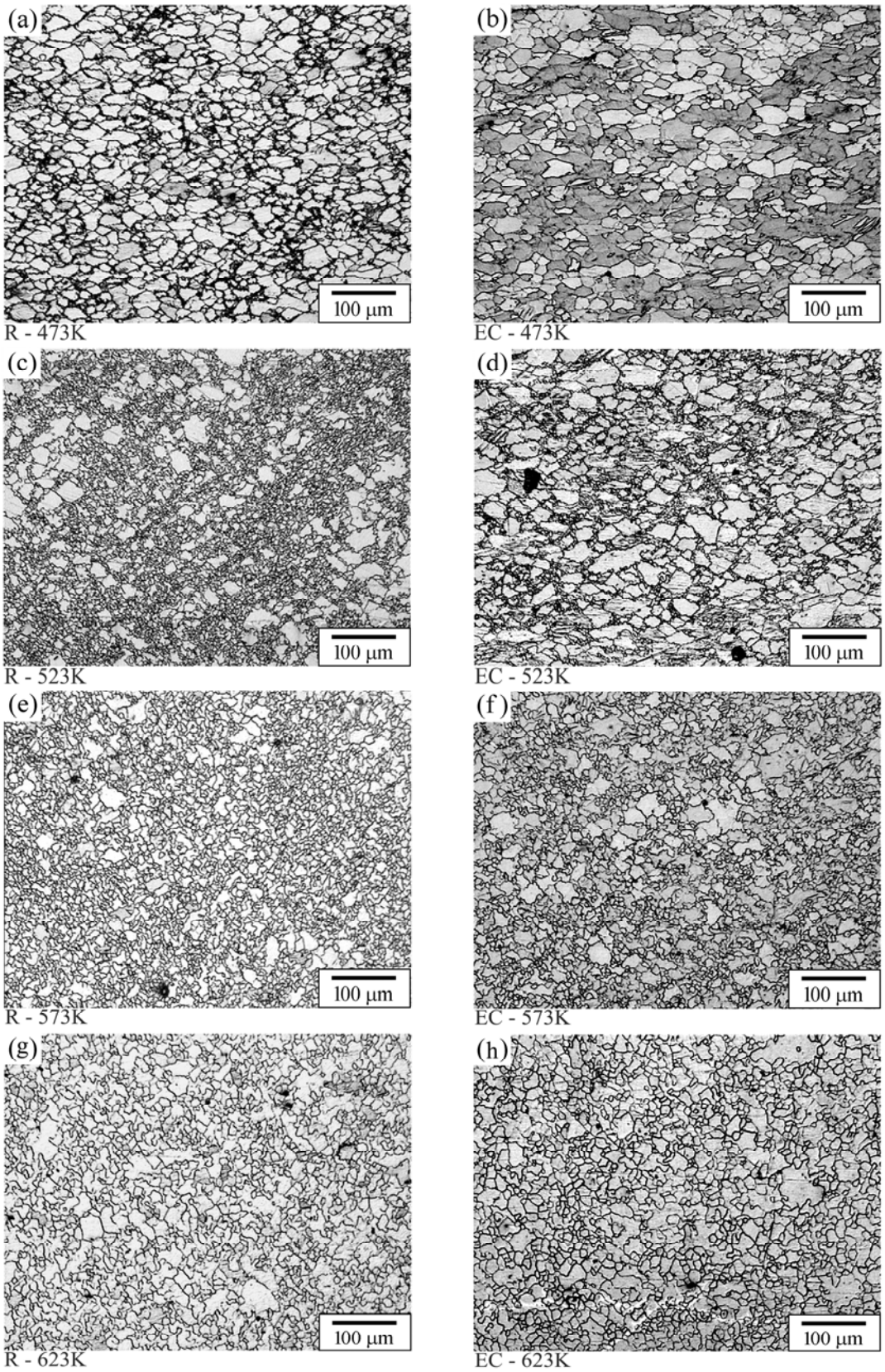

Figure 4: Optical micrographs of R and EC samples tested to ε = 0.4, at temperatures in the range 473 to 623 K

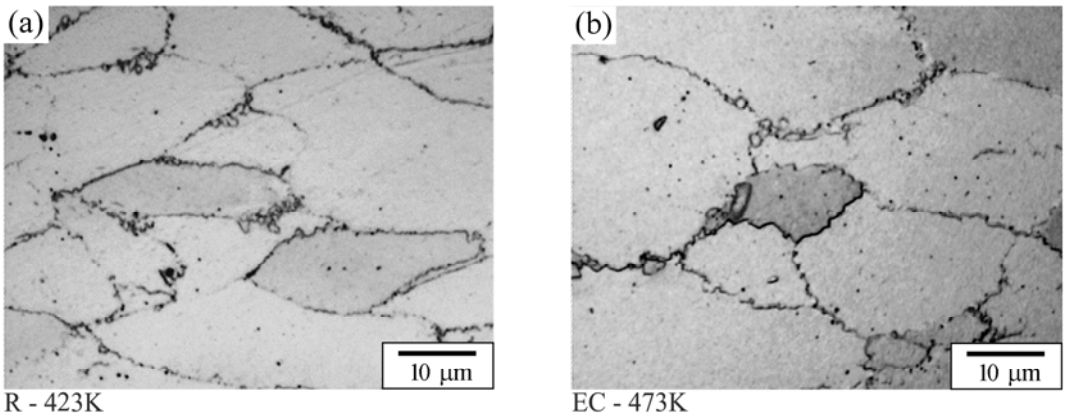

Figure 5: Examples of recrystallization at low temperature seen at higher magnification, for R and EC samples tested at 423 and 473 K respectively.

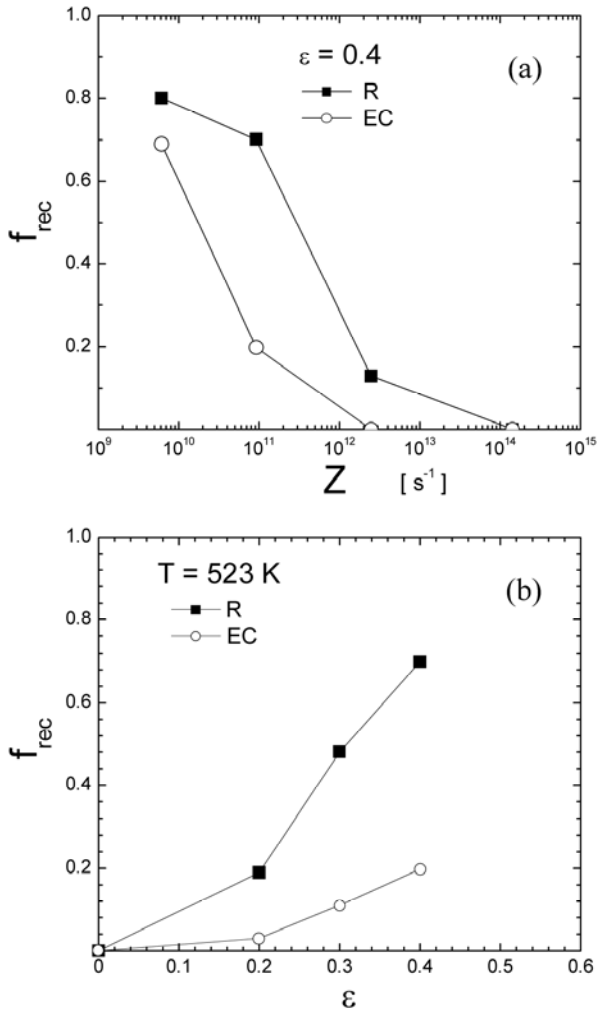

Figure 6: (a) The recrystallized volume fraction, f_{rec}, measured at $\varepsilon \approx 0.4$, as a function of the Zener-Hollomon parameter for R and EC samples. (b) The evolution of f_{rec} with strain for R

and EC samples at a constant temperature of 523 K.

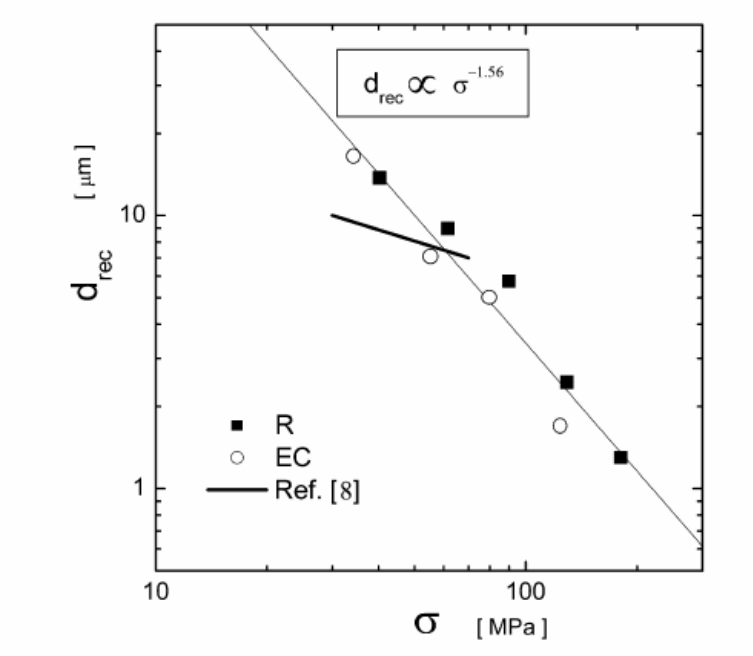

Figure 7: The recrystallized grain size, d_{rec}, is represented as a function of the maximum stress and

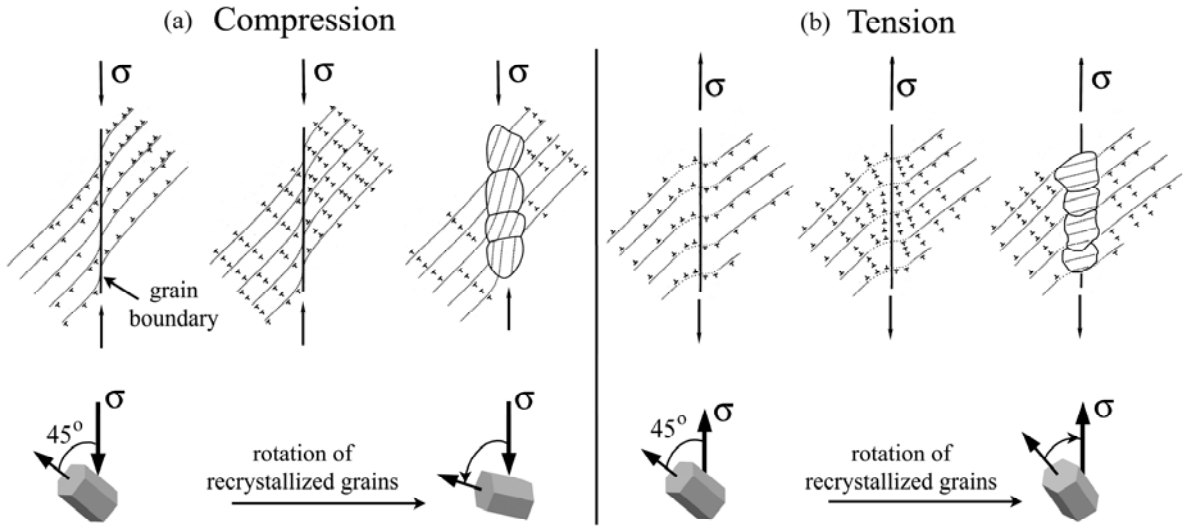

Figure 8: The rotation of recrystallized grains, as predicted by the RDRX model, during: (a) compression test (b) tensile test.

References

[1] S.E. Ion, F.J. Humphreys, S.H. White, Acta Metall. 30 (1982) 1909-1919.
[2] F.J. Humphreys, M. Hatherly, Recrystallization and Related Annealing Phenomena, second ed., Elsevier, Oxford, UK, 2004.
[3] A. Galiyev, R. Kaibyshev, G. Gottstein, Acta Mater. 49 (2001) 1199-1207.
[4] O. Sitdikov, R. Kaibishev, Mater Trans. 42 (2001) 1928-1937.
[5] A. Mwembela, E.B. Konopleva, H.J. McQueen, Scripta. Mater. 37 (1997) 1789-1795.
[6] M.M. Myshlyaev, H.J. McQueen, A. Mwembela, E. Konopleva. Mater. Sci. Eng. A337 (2002) 121-133.
[7] M.R. Barnett, J. Light Metals. 1 (2001) 167-177.
[8] M.R. Barnett, Mater. Trans. 44 (2003) 571-577.
[9] A.G. Beer, M.R. Barnett, Mater. Sci. Eng. A423 (2006) 292-299.
[10] M.R. Barnett, A.G. Beer, D. Atwell, A. Oudin, Scripta Mater. 51 (2004) 19-24.
[11] B. Derby, Acta Metall Mater. 39 (1991) 955-962.
[12] S.B. Yi, S. Zaefferer, H.G. Brokmeier, Mater. Sci. Eng. A424 (2006) 275-281.
[13] J.A. del Valle, F. Carreño, O.A. Ruano,Acta Mater. 54 (2006) 4247-4259
[14] J.A. del Valle, O.A. Ruano, Acta Mater. 55 (2007) 455-466.
[15] J.A. del Valle, M.T. Pérez-Prado, O.A. Ruano. Metall. Mater. Trans. A, 36 (2005) 1427-1438.
[16] R.Z. Valiev, R.K. Islamgaliev, I.V.Alexandrov, Prog. Mater. Sci. 45 (2000) 103.
[17] Q. Guo, H.G. Yang, H. Zhang, Z.H. Chen, Z.F. Wang, Mater. Sci. Tech. 21 (2005) 1349-1354.
[18] J.A. del Valle, F. Peñalba, O.A. Ruano, Mater. Sci. Eng. A467 (2007) 165-171.
[19] S.B. Yi, C.H.J. Davies, H.G. Brokmeier, R.E. Bolmaro, K.U. Kainer, J. Homeyer, Acta Mater. 54 (2006) 549-562.
[20] O.A. Ruano, O.D. Sherby, Revue Phys. Appl. 23 (1988) 625-637.
[21] O.A. Ruano, A.K. Miller, O.D. Sherby, Mater. Sci. Eng. 51 (1981) 9-16.
[22] S.S. Vagarali, T.G. Langdon, Acta Metall. 29 (1981) 1969-1982.
[23] W.J. Kim, S.W. Chung, C.S. Chung, D. Kum, Acta Mater. 49 (2001) 3337-3345.
[24] G.R. Edwards, T.R. McNelley, O.D. Sherby, Scripta Metall. 8 (1974) 475-479.